

Toughening effect of CPE on ASA/SAN binary blends at different temperatures

Zepeng Mao, Jun Zhang

Department of Polymer Science and Engineering, College of Materials Science and Engineering, Nanjing Tech University, Nanjing 210009, China

Correspondence to: J. Zhang (E-mail: zhangjun@njtech.edu.cn)

ABSTRACT: The effect of chlorinated polyethylene (CPE) on the impact toughness of acrylonitrile–styrene–acrylic (ASA) terpolymer/styrene–acrylonitrile copolymer (SAN) binary blends (25/75, w/w) was systematically investigated at three different temperatures ($-30\text{ }^{\circ}\text{C}$, $0\text{ }^{\circ}\text{C}$, and $23\text{ }^{\circ}\text{C}$). With the addition of 60 phr CPE, the impact strength increased by 11 times at $23\text{ }^{\circ}\text{C}$ and 10 times at $0\text{ }^{\circ}\text{C}$. However, the toughening effect was not obvious when the testing temperature was $-30\text{ }^{\circ}\text{C}$. Since the glass-transition temperature (T_g) of CPE was about $-18.3\text{ }^{\circ}\text{C}$ as measured with dynamic mechanical analysis tests, the polymeric chains of CPE have been “frozen out” at $-30\text{ }^{\circ}\text{C}$. As a result, CPE evidently cannot improve the toughness of the blend system. The morphology of impact-fractured surfaces observed by scanning electron microscopy also confirmed the effect of CPE on the impact toughness of ASA/SAN binary blends. The heat distortion temperature remained almost unchanged, indicating that the improvement in toughness did not sacrifice heat resistance. Furthermore, other mechanical properties were evaluated, and the possible interactions among components of the blends were also analyzed by Fourier transform infrared spectra. © 2016 Wiley Periodicals, Inc. *J. Appl. Polym. Sci.* **2016**, *133*, 43353.

KEYWORDS: blends; copolymers; glass transition; properties and characterization

Received 29 August 2015; accepted 19 December 2015

DOI: 10.1002/app.43353

INTRODUCTION

Acrylonitrile–styrene–acrylic (ASA) terpolymer is a typical core–shell structured polymer, which is obtained by grafting copolymerization of styrene and acrylonitrile monomers onto cross-linked poly(*n*-butyl acrylate) (PnBA) particles.^{1,2} The structures of ASA and ABS (acrylonitrile–butadiene–styrene) are similar. They have the same styrene–acrylonitrile graft shells, but the polybutadiene (PB) rubber core within the ABS is substituted by the PnBA rubber core in the ASA. Compared with the butadiene rubber core of ABS, ASA performed with outstanding weather resistance^{3–5} by virtue of no incorporation of double bonds in the main chains of the acrylic elastomer core. Styrene–acrylonitrile (SAN) copolymer is a rigid material at room temperature for which the glass-transition temperature is higher than $100\text{ }^{\circ}\text{C}$.⁶ To enhance the impact toughness of SAN, ASA is often introduced into a SAN system to prepare ASA/SAN binary blends, which have excellent rigidity, heat resistance, and advanced weather resistance. A good compatibility exists in the ASA/SAN binary blends because SAN is the shell of ASA. However, as reported in the literature,⁷ the use of ASA fails to give a significant increase in the toughness of brittle SAN, even when the concentration is over 30%. Therefore, improving the impact toughness of ASA/SAN binary blends is of great importance.

CPE is an impact modifier of long reputation that is often introduced into other polymers to improve toughness, and it has other properties like oil resistance and flame retardancy. As reported, CPE has been applied to toughen many different polymers, such as HDPE,⁸ PVC,^{9–12} and PMMA.¹³ Furthermore, the mechanical properties, rheological properties, morphology, and thermomechanical degradation of CPE/SAN,^{14–16} CPE/ASA,¹⁷ CPE/PVC/SAN,¹⁸ and PVC/SAN¹⁹ blends were investigated in the literature, which found a good compatibility and a high toughening efficiency. Thus it is reasonable to choose CPE to toughen the ASA/SAN binary blends.

In fact, when some polymer materials are used outdoors or in winter, the service temperature is often far below room temperature ($23\text{ }^{\circ}\text{C}$). Thus, it would be of great interest to study the toughness of polymer materials at $23\text{ }^{\circ}\text{C}$, even under the ice point. The toughness of ASA/SAN/CPE blends at lower temperatures has barely been investigated in the literature.

In this paper, the impact toughness of ASA/SAN/CPE (25/75/0–60, w/w/w) blends was investigated at three different temperatures ($-30\text{ }^{\circ}\text{C}$, $0\text{ }^{\circ}\text{C}$, and $23\text{ }^{\circ}\text{C}$), as well as the tensile strength, the flexural properties, and the heat distortion temperature (HDT). Dynamic mechanical analysis (DMA) and scanning electron microscopy (SEM) were also conducted to better propose

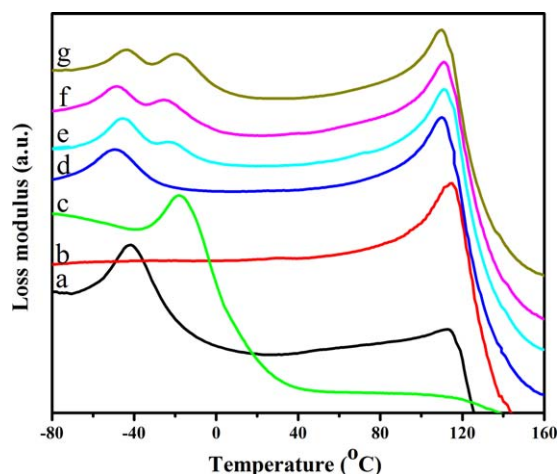


Figure 1. Loss modulus (G'') as a function of temperature for ASA/SAN/CPE ternary blends: (a) 100/0/0, (b) 0/100/0, (c) 0/0/100, (d) 25/75/0, (e) 25/75/10, (f) 25/75/20, and (g) 25/75/30. [Color figure can be viewed in the online issue, which is available at wileyonlinelibrary.com.]

the toughening mechanism. The possible interactions among components of the blends were also analyzed by Fourier transform infrared (FTIR) spectra.

EXPERIMENTAL

Materials

ASA (HX-960) was supplied by Zibo Huaxing Additives Co., Zibo, China. SAN (D-178) was supplied by Zhenjiang GPPC Chemical Co., Zhenjiang, China. CPE (135A), with 36 wt % of chloride, was produced by Weifang Yaxing Chemical Co., Weifang, China.

Sample Preparation

ASA, SAN, and CPE were mixed by a two-roll mill at 180 °C for 10 min. The blends were subsequently compression-molded into sheets of 2 and 4 mm thickness at 180 °C. Dumbbell-shaped specimens cut from 2 mm sheets were used for the tensile test. Rectangular specimens (80 × 10 × 4 mm³) cut from sheets with 4 mm thickness were prepared for the flexural, impact, and heat distortion temperature tests.

Glass-Transition Temperature

The glass-transition temperature of the ASA/SAN/CPE ternary blends was determined by a modular compact rheometer (MCR302, Anton Paar, Graz, Austria). The dynamic mechanical analysis of the blends was scanned in a torsion mode with a frequency of 1 Hz in the temperature range from -90 °C to 160 °C at a heating rate of 3 °C/min. The dimensions of each specimen were 30 × 6 × 2 mm³. The T_g was defined as the peak of the $\tan \delta$ and loss modulus (G'') curves.

Impact Properties

The notched Izod impact tests were carried out on an Izod impact apparatus (UJ-4, Chengde Machine Factory, Chengde, China), following ISO 180. Each test was conducted at three different temperatures (-30 °C, 0 °C, and 23 °C). Before testing, the specimens were kept at the corresponding temperature for 10 hours in order to rule out any temperature errors. The test at 23 °C was conducted in an air-conditioned room. For the tests at 0 °C and -30 °C, the samples were first cooled for 10 hours in a refrigerator

where the temperature had already been set, and then the samples were taken out of the refrigerator to test instantly.

Scanning Electron Microscopy Analysis

The impact-fractured surfaces were observed by a scanning electron microscope (JSM-5900, JEOL, Tokyo, Japan) with an accelerating voltage of 15 kV. The fractured surfaces were coated with a conductive layer of gold before viewing.

Flexural and Tensile Properties

The flexural and tensile tests were conducted on a universal testing machine (CMT 5254, Shenzhen SANS Testing Machine Co., Shenzhen, China) with an invariant rate of 2 and 5 mm/min, according to ISO 178 and ISO 527, respectively. Both tests were performed at room temperature (23 °C).

Heat Distortion Temperature

The heat distortion temperature of the ASA/SAN/CPE ternary blends was evaluated by using Vicat/HDT equipment (ZWK 1302-2, Shenzhen SANS Testing Machine Co.). All tests were conducted under the maximum bending stress of 1.80 and 0.45 MPa with a heating rate of 120 °C/h, following ISO 75-2.

Fourier Transform Infrared Spectroscopy Analysis

Fourier transform infrared spectra were used to investigate the interaction between the components of the ASA/SAN/CPE ternary blend system. The spectra of the specimens (<30 μm) were obtained on an FTIR spectrometer (Nicolet iS5, Thermo Fisher, Waltham, USA) with a resolution of 4 cm⁻¹.

RESULTS AND DISCUSSION

Glass-Transition Temperature

DMA was used to analyze the glass-transition behaviors of the ASA/SAN/CPE ternary blends. The $\tan \delta$ curves and G'' curves of the ASA, SAN, CPE, and ASA/SAN/CPE ternary blends are shown in Figures 1 and 2. The peak temperatures of the $\tan \delta$ and G'' curves are referred to as the T_g of the corresponding components, the values of which are listed in Table I.

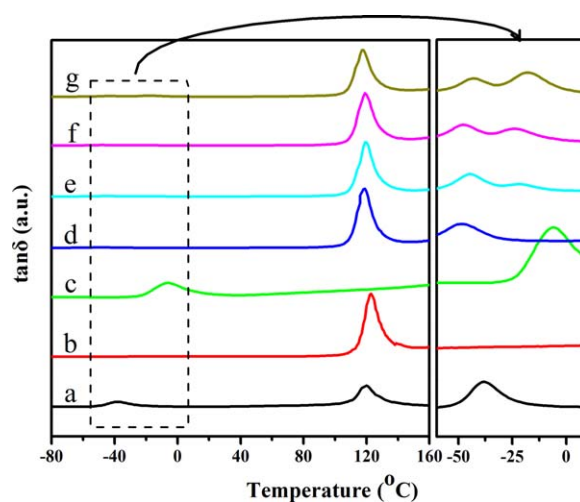


Figure 2. $\tan \delta$ as a function of temperature for ASA/SAN/CPE ternary blends: (a) 100/0/0, (b) 0/100/0, (c) 0/0/100, (d) 25/75/0, (e) 25/75/10, (f) 25/75/20, and (g) 25/75/30. [Color figure can be viewed in the online issue, which is available at wileyonlinelibrary.com.]

Table I. Glass-Transition Temperature of ASA/SAN/CPE Ternary Blends from G'' and $\tan \delta$ Curves

Sample	G''			$\tan \delta$		
	$T_{g,1}$ (°C)	$T_{g,2}$ (°C)	$T_{g,3}$ (°C)	$T_{g,1}$ (°C)	$T_{g,2}$ (°C)	$T_{g,3}$ (°C)
ASA	-41.4	—	112.8	-38.0	—	119.6
SAN	—	—	114.6	—	—	122.8
CPE	—	-18.3	—	—	-6.3	—
ASA/SAN/CPE						
25/75/0	-49.4	—	110.3	-48.3	—	118.7
25/75/10	-45.9	-23.0	111.4	-45.0	-21.9	119.7
25/75/20	-48.3	-24.9	111.4	-47.2	-23.9	118.6
25/75/30	-43.8	-20.0	110.3	-42.9	-17.9	117.6

In Figures 1 and 2, SAN and CPE show only one glass-transition temperature, while two are detected in ASA. ASA is obtained by grafting the copolymer of SAN onto PnBA rubber particles, which means the T_g in the low-temperature region (-41.4 or -38.0 °C) is attributed to the PnBA core, and the T_g in the high-temperature region (112.8 or 119.6 °C) corresponds to the SAN shell of ASA.

All ternary blends of ASA/SAN/CPE show three T_g s: one is in the high-temperature region (corresponding to the SAN segment), and two are in the low-temperature region (corresponding to CPE and the PnBA core of ASA).

As shown in Table I, the T_g s of the pure CPE (-6.3 °C) and the CPE (-21.9 °C to -17.9 °C) component of blends that are obtained from the $\tan \delta$ curves show a significant deviation. The same phenomenon has been reported previously.^{14,20} One explanation is that the negative pressure is created by the difference in thermal expansion coefficients of the soft and hard phases.²¹ However, the T_g s of pure CPE (-18.3 °C) and the CPE (-24.9 °C to -20.0 °C) component of blends that are obtained from the G'' curves are roughly equal. Therefore, in this study, the peak temperatures of the G'' are chosen to define the T_g s of the corresponding components too.²² In addition, other T_g s obtained from G'' curves are approximately equal to the T_g s obtained from the $\tan \delta$ curves in the low-temperature region (<0 °C) and have a gap of about 7–8 °C in the high-temperature region (>0 °C).

Compared with the T_g s observed in the ASA/SAN/CPE ternary blends, all of the T_g s show no obvious vibration in the high-temperature region. With respect to the T_g s of the ASA/SAN/CPE (25/75/0–60) blends in the low-temperature region, the values of $T_{g,1}$ increase slightly in the presence of CPE. The addition of CPE may restrain the movement of the rubber phase at temperatures lower than -18.3 °C. Therefore, the more CPE is added, the more obvious is the restraint effect.

Impact Property

The impact test is an important measurement to characterize the toughness of a polymer material, which is also the key factor to be considered in this study. The impact strengths of the ASA/SAN/CPE ternary blends are measured at three different temperatures (-30 °C, 0 °C, and 23 °C), and the results are exhibited in Figure 3. When the test is conducted at room tem-

perature (23 °C), the addition of CPE effectively improves the toughness of the ASA/SAN (25/75) blends, and a ductile–brittle transition of impact strength is observed at 10–25 phr CPE. It can be seen that the ASA/SAN (25/75) blends have a poor toughness with an impact strength of 4.88 kJ/m², while the strength increases with further increasing CPE content. For example, when 60 phr CPE is added, the impact strength increases to 58.05 kJ/m², which is nearly 11 times higher than for the pure ASA/SAN (25/75) blends, indicating the high toughening efficiency of CPE in this system.

Considering the ASA/SAN/CPE blends at a temperature of 0 °C, when 60 phr CPE is introduced, the impact strength increases from 4.29 kJ/m² to 49.14 kJ/m², which is still 10 times higher than the blends without CPE. A transition is found to occur in the range of 30–40 phr of CPE. Though the impact strength does not reach the level of 23 °C, the toughening effect is still quite obvious.

Interestingly, when the test is performed at -30 °C, the addition of CPE into ASA/SAN (25/75) blends does not influence the impact strength distinctly compared to when at 23 °C and 0 °C. The impact strength of the ASA/SAN/CPE ternary blends hardly increases even when 25 phr CPE is added, and a weak transition is shown at 30–40 phr CPE.

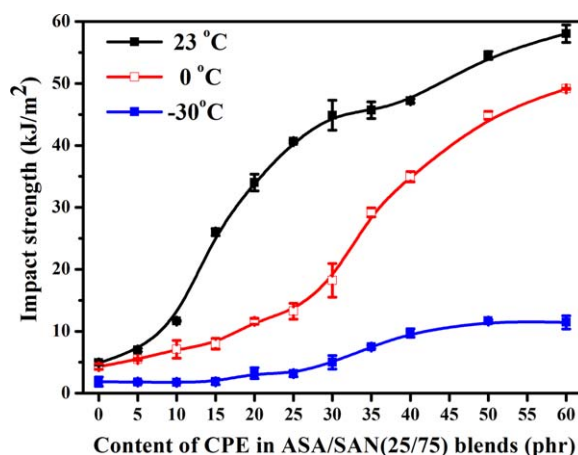


Figure 3. Impact strength of ASA/SAN/CPE (25/75/0–60) ternary blends at different temperatures. [Color figure can be viewed in the online issue, which is available at wileyonlinelibrary.com.]

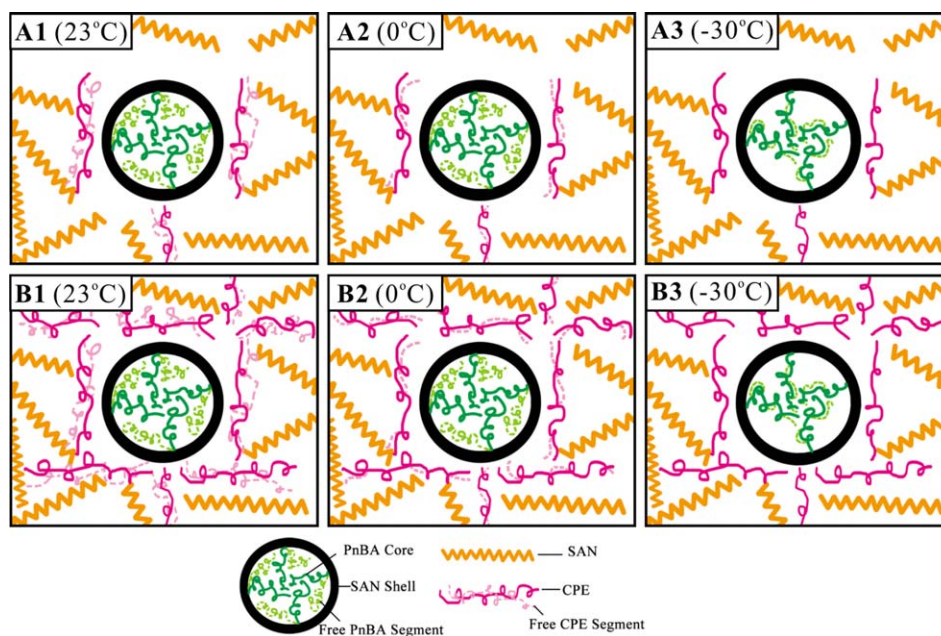


Figure 4. Schematic presentation for the toughening mechanism of CPE at different temperatures: (A1, A2, A3): ASA/SAN/CPE (25/75/5); (B1, B2, B3): ASA/SAN/CPE (25/75/30). [Color figure can be viewed in the online issue, which is available at wileyonlinelibrary.com.]

The toughening mechanism is proposed in Figure 4. The spherical structure represents the ASA, the black circular shell is the SAN shell, and the green random coil structure is the PnBA core. The orange rigid chain structure represents the SAN matrix. The red random coil structure is CPE. In addition, the light green and pink dash structures represent the free PnBA segments and the free CPE segments, respectively. As reported in the early literature,^{23,24} the toughening mechanism of CPE is that some CPE network structures formed in the polymer matrix. From the result of the DMA analysis, the T_g of CPE is below -6 °C. Therefore, CPE is in a rubbery state at room temperature (23 °C), where the CPE molecular chains have a great deal of freedom to move and take up all of the conformations. When the CPE proportion is low (shown in Figure 4, A1), the limited number of CPE particles are isolated and fail to form a continuous network. However, after the CPE content increases to a certain extent (shown in B1), there would be a continuous network in the matrix, and the impact energy is effectively dissipated or released through the CPE network. Hence, the impact strength of the blends grows noticeably. When the testing temperature drops to 0 °C, which is close to the T_g of CPE, the movement of most CPE segments is restricted, and only a portion of the segments are free to move (shown in A2 and B2). Whether the CPE content is low or high, the testing results cannot reach the level of 23 °C. At the temperature below T_g (-30 °C), CPE is in a glassy state, and all the soft chains are “frozen out”; thus the CPE becomes a rigid polymer and can hardly improve the toughness of ASA/SAN (25/75) blends (shown in A3 and B3). In addition, -30 °C is close to the T_g of PnBA (the core of ASA), so only some PnBA segments are free to move. Based on the two reasons mentioned above, the impact strength of the blends is not enhanced but is maintained at lower than 10 kJ/m².

SEM Analysis

An SEM analysis is usually performed to visualize the morphology of materials. The SEM micrographs of impact-fractured surfaces at different temperatures are exhibited in Figure 5. There is no obvious phase separation in the blend system, indicating that the components of ASA/SAN/CPE ternary blends are compatible, which correlates well with the aforementioned DMA results. It can be observed that the impact-fractured surfaces are rougher and rougher with increasing CPE proportion and temperature. The SEM image of the ASA/SAN/CPE (25/75/30) blend at 23 °C shows a rough surface, indicating good toughness. In contrast, the ASA/SAN/CPE (25/75/30) blend of -30 °C shows a relatively smooth surface, implying brittle fracture. The reason for this result is that the chains of CPE are “frozen out,” and there is no toughening effect in the matrix. A detailed discussion of the toughening mechanism has been introduced in the Figure 4.

In addition, in the SEM photos, there are no microholes in the ASA/SAN pure matrix at 23 °C. However, the porous surface is formed when 10–20 phr CPE is introduced where the impact strength is also in a rapid-increase stage from Figure 3. This is mainly because that limited content of CPE fails to form a continuous network. When samples are impacted to fracture, a noncontinuous network cannot dissipate the energy evenly, so some microporous structures are developed at stress-concentrative points of the CPE network. Furthermore, after the CPE content increases to 30 phr, a continuous network emerges, and the impact energy is released uniformly through the continuous CPE network. Therefore the microholes in the surface disappear again.

Tensile and Flexural Properties

The stress–strain curves of ASA/SAN/CPE ternary blends are acquired at 23 °C and are shown in Figure 6. With the addition

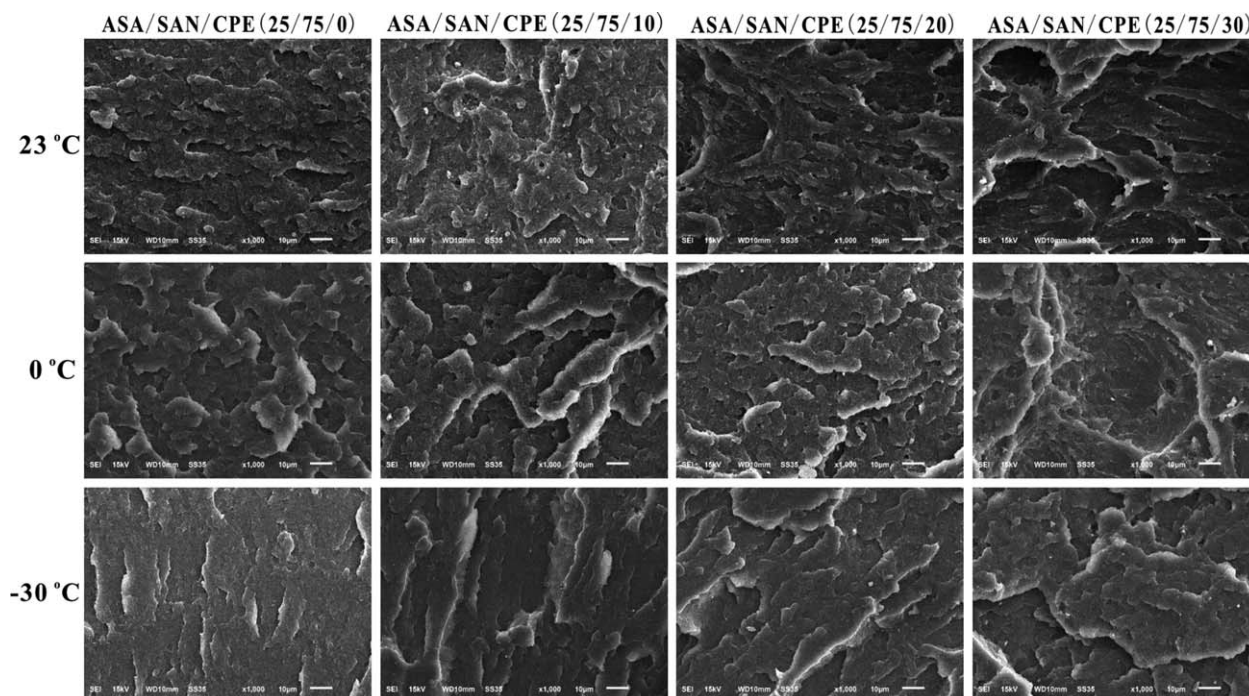


Figure 5. SEM photographs of ASA/SAN/CPE ternary blends.

of CPE, the elongation at break increases while tensile strength decreases. The decrease in tensile strength is mainly due to the low strength and modulus of CPE.^{10,23} The tensile strength of the blends would decrease when a large amount of CPE is added. The tensile strength is still more than 30 MPa after 30 phr CPE is added. However, when more than 30 phr of CPE is added, the yield strength of the blends decreases in a large scale. The elongation at break is another factor that can characterize the toughness of materials.²³ In this study, the elongation at break grows from 13% to 141%, indicating that the toughness of the blends is improved with the increase of CPE content. The results of elongation at break are consistent with the results of the impact strength.

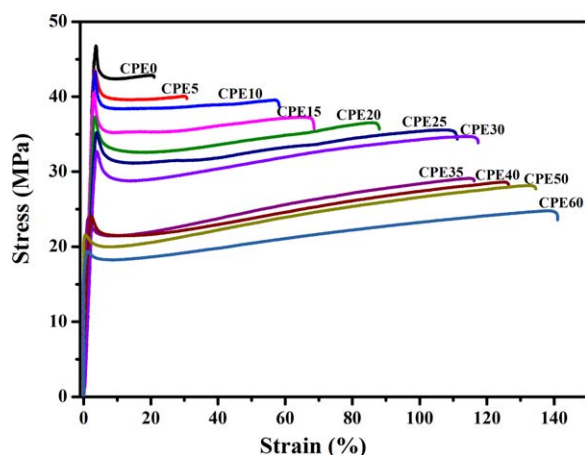


Figure 6. Tensile stress-strain curves of ASA/SAN/CPE (25/75/0–60) ternary blends. [Color figure can be viewed in the online issue, which is available at wileyonlinelibrary.com.]

In general, when the CPE is used as the toughening modifier for rigid plastics, the flexural properties are supposed to decline.²³ The flexural properties of ASA/SAN/CPE blends are shown in Figure 7. Both flexural strength and flexural modulus decrease by adding more CPE. When 30 phr CPE is added, the flexural strength and flexural modulus decline by 37% and 34%, respectively. Flexural properties are usually used to evaluate the stiffness of the materials, and the decline of the flexural strength indicates the decrease of stiffness of the blends.

Heat Distortion Temperature

The HDT results of ASA/SAN/CPE ternary blends are shown in Figure 8. Interestingly, the addition of CPE has little influence on the HDT of ASA/SAN (25/75) blends: all of the HDTs

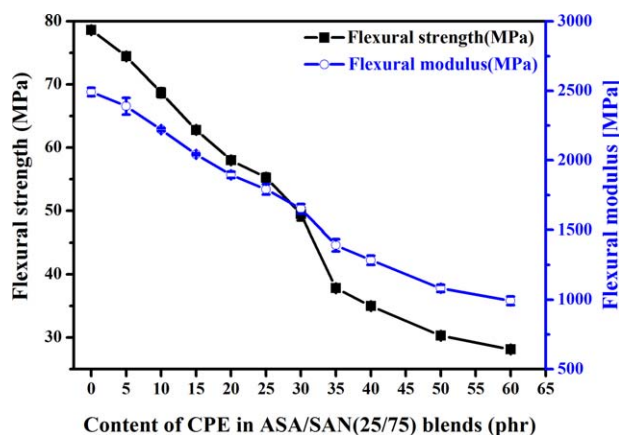


Figure 7. Flexural properties of ASA/SAN/CPE (25/75/0–60) ternary blends. [Color figure can be viewed in the online issue, which is available at wileyonlinelibrary.com.]

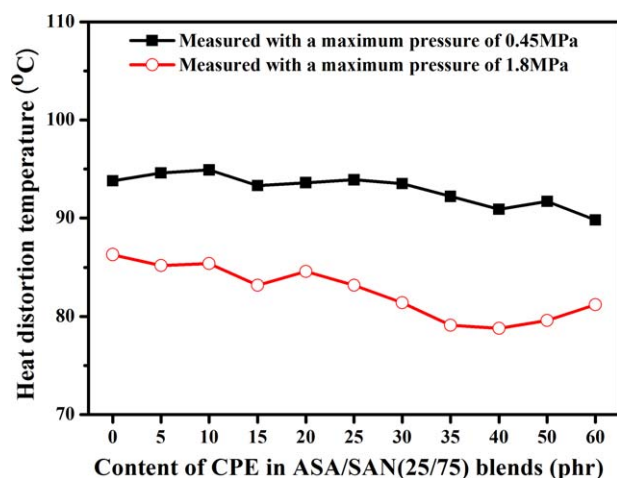


Figure 8. Heat distortion temperatures of unannealed ASA/SAN/CPE (25/75/0–60) ternary blends. [Color figure can be viewed in the online issue, which is available at wileyonlinelibrary.com.]

measured under the maximum pressure of 0.45 MPa are above 90 °C and drop a little, and the HDT measured under the maximum pressure of 1.8 MPa decreases only 5.1 °C when adding 60 phr CPE.

This result may be attributed to the 75 phr SAN content: SAN is a resin with relatively high stiffness, and it is effective in enhancing the HDT of the blends.⁷ Since the ternary blends are SAN-rich blends, the addition of CPE could only decrease the HDT on a limited scale. Similar results have been reported in our previous research.²⁵

FTIR Spectra Analysis

The FTIR spectra of ASA/SAN/CPE ternary blends composed of different weight ratios are shown in Figure 9. The carbonyl (C=O) and cyano (C≡N) stretching appear at 1736 cm^{-1} and 2238 cm^{-1} , respectively. The bands at 701 cm^{-1} and 1602 cm^{-1} are characteristic peaks of a single-substituted phenyl ring and the vibration of a benzene skeletal ring, respectively. Moreover, bands at 2925 cm^{-1} , 2850 cm^{-1} , and 1453 cm^{-1} are associated

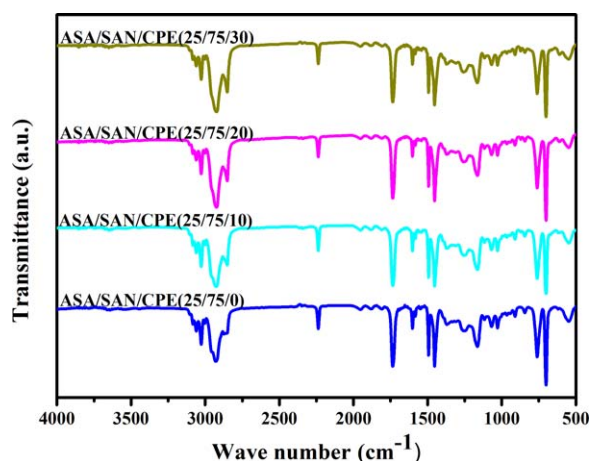


Figure 9. FTIR spectra of ASA/SAN/CPE ternary blends. [Color figure can be viewed in the online issue, which is available at wileyonlinelibrary.com.]

with the C—H asymmetric stretching and symmetric stretching and the bending vibration of $-\text{CH}_2-$, respectively. The C—H symmetric stretching and the bending of $-\text{CH}_3$ are at 2870 cm^{-1} and 1380 cm^{-1} , respectively. In addition, the characteristic peaks of CPE with random chlorination of about 36 wt % are expected to be similar to poly(vinyl chloride).²⁶ Here, a weak stretching peak for C—Cl at 709 cm^{-1} ²⁷ is overlapped by the strong peaks of a single-substituted phenyl ring. However, no obvious shift of wave number of the main groups is observed in the FTIR spectra, indicating the nonexistence of strong specific intermolecular interactions in ASA/SAN/CPE ternary blends. Thus the addition of CPE to ASA/SAN binary blends is a physical action.

CONCLUSIONS

ASA/SAN/CPE (30/70/0–60) ternary blends were prepared by melt blending. A DMA analysis showed that the blends had three T_g s: two were in the low-temperature region and another was in the high-temperature region. The addition of CPE was effective in improving the impact toughness of ASA/SAN (25/75) blends at 23 °C and 0 °C, but the impact strength of the blends increased little at -30 °C. This conclusion was verified by SEM: the impact-fractured surface of the ASA/SAN/CPE (25/75/30) blend was rough at 23 °C and 0 °C, while the impact-fractured surface of the ASA/SAN/CPE (25/75/30) blend was relatively smooth at -30 °C. The tensile strength and flexural properties decreased with the increase of CPE, yet the HDT of ASA/SAN/CPE (25/75/0–60) blends hardly changed. Furthermore, the FTIR analysis demonstrated that no strong interactions existed in the ternary blends. According to the results obtained in this work, the toughening effect of 30 phr CPE was not perceptible at -30 °C. Hence, in further research, work to further improve the toughness of ASA/SAN blends at -30 °C will be attempted.

ACKNOWLEDGMENTS

This work was supported by the Priority Academic Program Development of Jiangsu Higher Education Institutions (PAPD).

REFERENCES

- Tolue, S.; Moghbeli, M. R.; Ghafelebashi, S. M. *Eur. Polym. J.* **2009**, *45*(3), 714.
- Shi, X. Z.; Cheng, W. Z.; Lu, Z. X.; Du, Q. G.; Yang, Y. L. *Polym. Bull.* **2002**, *48*(4–5), 389.
- Du, Y. G.; Gao, J. G.; Yang, J. B.; Liu, X. Q. *J. Polym. Res.* **2012**, *19*(11), 9993.
- Han, Y.; Tai, Z. X.; Zhou, C.; Zhang, M. Y.; Zhang, H. X.; Liu, F. Q. *Polym. Bull.* **2009**, *62*(6), 855.
- Datta, P.; Guha, C.; Sarkhel, G. *Polym. Adv. Technol.* **2014**, *25*(12), 1454.
- Modesti, M.; Besco, S.; Lorenzetti, A.; Zammarano, M.; Causin, V.; Marega, C.; Gilman, J. W.; Fox, D. M.; Trulove, P. C.; De Long, H. C.; Maupin, P. H. *Polym. Adv. Technol.* **2008**, *19*, 1576.

7. Zhang, W.; Chen, S. J.; Zhang, J. J. *Thermoplast. Compos.* **2013**, 26(3), 322.
8. Chaudhry, A. U.; Mittal, V. *Polym. Eng. Sci.* **2014**, 54(1), 85.
9. Du, Z. A.; Xu, C.; Zhao, Z. Q.; Zhao, J. R.; Feng, Y. J. *Appl. Polym. Sci.* **2011**, 121(1), 86.
10. Eastwood, E. A.; Dadmun, M. D. *Polymer* **2002**, 43(25), 6707.
11. Klaric, I.; Vrandecic, N. S.; Roje, U. *J. Appl. Polym. Sci.* **2000**, 78(1), 166.
12. Zhong, Z. K.; Zheng, S. X.; Yang, K. J.; Guo, Q. P. *J. Appl. Polym. Sci.* **1998**, 69(5), 995.
13. Ueda, H.; Karasz, F. E. *Polym. J.* **1994**, 26(7), 771.
14. Hwang, I. J.; Kim, B. K. *J. Appl. Polym. Sci.* **1998**, 67(1), 27.
15. Hwang, I. J.; Lee, M. H.; Kim, B. K. *Eur. Polym. J.* **1998**, 34(5–6), 671.
16. Luo, P.; Wu, G. Z. *Polym. Degrad. Stabil.* **2012**, 97(5), 766.
17. Zhang, Z.; Zhu, W.; Zhang, J.; Tian, T. *Polym. Test.* **2015**, 44, 23.
18. Yang, W. J.; Wu, Q. Y.; Zhou, L. L.; Wang, S. Y. *J. Appl. Polym. Sci.* **1997**, 66(8), 1455.
19. Kim, J. H.; Barlow, J. W.; Paul, D. R. *J. Polym. Sci., Part B: Polym. Phys.* **1989**, 27(11), 2211.
20. Zhang, Z.; Zhao, X. J.; Zhang, J.; Chen, S. J. *Compos. Sci. Technol.* **2013**, 86, 122.
21. Wang, R. W.; Wang, W. J. *J. Appl. Polym. Sci.* **2003**, 90(8), 2260.
22. Ma, P. *Express Polym. Lett.* **2014**, 8(7), 517.
23. Zhang, Z.; Chen, S. J.; Zhang, J.; Li, B.; Jin, X. P. *Polym. Test.* **2010**, 29(8), 995.
24. Siegmann, A.; Hiltner, A. *Polym. Eng. Sci.* **1984**, 24(11), 869.
25. Zhang, W.; Zhang, J.; Chen, S. J. *J. Mater. Sci.* **2012**, 47(12), 5041.
26. Fekete, E.; Foldes, E.; Pukanszky, M. *Eur. Polym. J.* **2005**, 41(4), 727.
27. Bhagabati, P.; Chaki, T. K. *J. Appl. Polym. Sci.* **2014**, 131(11), 40316.